[redacted]

NRL Report 5056
Copy No. 119

UNCLASSIFIED

ANALYTICAL DETERMINATION OF AIRBORNE RADAR RESPONSE TO EXTRANEOUS INPUTS

[[redacted]]

Charles F. White and C. M. Loughmiller

Equipment Research Branch
Radar Division

December 18, 1957

[redacted]

[redacted]

DECLASSIFIED: By authority of
OPNAVINST 5510.1H, 29 APR 88
Cite Authority Date
C. ROGERS 1221.1
Entered by NRL Code

NAVAL RESEARCH LABORATORY
Washington, D.C.

APPROVED FOR PUBLIC RELEASE
DISTRIBUTION UNLIMITED

[redacted]

PLEASE RETURN THIS COPY TO:
NAVAL RESEARCH LABORATORY
WASHINGTON, D.C. 20390
ATTN: CODE 2028

Because of our limited supply you are requested to return this copy as soon as it has served your purposes so that it may be made available to others for reference use. Your cooperation will be appreciated.

PRNC-NRL-20-820

[redacted]

[redacted]

[redacted]

[redacted].

[redacted]

[redacted]

UNCLASSIFIED

NRL Report 5056

ANALYTICAL DETERMINATION OF AIRBORNE RADAR RESPONSE TO EXTRANEOUS INPUTS

[redacted]

ANALYTICAL DETERMINATION OF AIRBORNE RADAR VULNERABILITY TO TARGET DISPENSED CHAFF AND REPEAT-BACK JAMMING

[redacted]

Charles F. White and C. M. Loughmiller

Equipment Research Branch
Radar Division

December 18, 1957

NAVAL RESEARCH LABORATORY
Washington, D.C.

[redacted]

[redacted]

UNCLASSIFIED

CONTENTS

[redacted]

A[redacted]

Airborne radar vulnerability to the countermeasures of target-dispensed chaff and repeat-back jamming are analytically determined using the AN/APQ-50 range- and angle-tracking servo system transfer functions as typical of current weapons control systems.

In all the calculations, the basic assumption is made that the jam-to-signal (J/S) ratio is very large. The chaff calculations establish the regions of successful employment under pure collision course dynamics with typical interceptor and target speeds.

To determine the theoretical minimum range pull-off time, an analog for the optimum transponder delay controller was evolved. Using the analog and the transfer function for the radar range servo, calculations were made of pull-off time corresponding to a wide range of J/S ratios. For the AN/APQ-50 radar, the calculated pull-off times range from 1/4 to 4 seconds for typical J/S ratios realizable in practice.

As an important side result of the study, an approach to the design of an optimum transponder delay controller is presented in which the initial delay is maintained throughout a range gate pull-off cycle.

PROBLEM STATUS

This report represents completion of one phase of the work; work is continuing.

AUTHORIZATION

NRL Problem R05-04
Projects NR 418-000, NR 418-001 and NA 431-009
BuAer No. EL-42001

Manuscript submitted October 22, 1957

[redacted]

UNCLASSIFIED

ANALYTICAL DETERMINATION OF AIRBORNE RADAR VULNERABILITY TO TARGET DISPENSED CHAFF AND REPEAT-BACK JAMMING

[[redacted]]

PART I - TARGET-DISPENSED CHAFF

INTRODUCTION

Radar receivers are protected from unwanted signals by the operation of other portions of the airborne fire control system. The antenna pattern is such that discrimination in angle (both train and elevation) is provided. Range gating provides a third dimension of discrimination. Close correspondence must be maintained between portions of the system in which the quantities target elevation angle, train angle, and range from the interceptor appear and the correct values are maintained by servo systems. Under the dynamic conditions of an airborne intercept (AI) attack, derivatives of these quantities enter into the servo system performance. The systems exhibit varying degrees of position, velocity, and acceleration memory.

Target dispensed chaff, the problem considered here, means the sudden appearance of an interfering signal within the volume defined by the position discrimination characteristics of the radar. Successful continuance of target tracking is the result of the combined action of the receiver AGC system and the radar servo systems. The AGC fast action hinders in the initial phase but aids later. The velocity memory characteristics of the servo systems become the principal aids in an effective "ignoring" of the interfering signal from the chaff. As seen later, velocity memeory or coast time is inversely proportional to the low frequency corner of the initial double integrator slope in the range servo system transfer characteristic.

PRELIMINARY CONSIDERATIONS

A pictorial depiction of the characteristics of the tactical situation and the degree to which the system utilizes these same characteristics to provide discrimination between target and unwanted signals would show (a) that the size of the target is recognized by the employment of angle and range discrimination to define a relatively small volume from which signals are accepted, and (b) that the motion of the target is recognized by servo systems designed to be capable of tracking under highly dynamic input conditions and simultaneously exhibiting velocity memory in the range coordinate.

The system performance for any radar will show the general characteristic with respect to jamming indicated in Fig. 1, where the jamming-to-signal ratio, and the differential between the jamming signal range rate and the target signal range rate are related. For a given J/S ratio any differential range rate to the left of the curve results in loss of range tracking. For any differential range rate to the right of the curve, the system continues to track the target.

With reference to Fig. 1, the calculations that follow provide only one value of $\Delta \dot{R}$. The value found corresponds to the J/S ratio associated with receiver saturation and has general applicability to the collision course used.

[redacted]

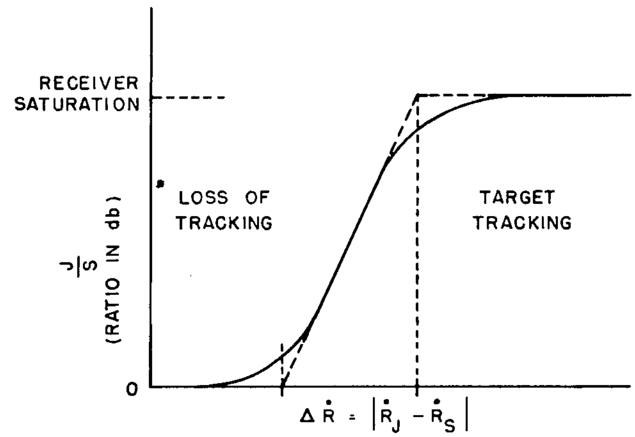

Fig. 1 - Jamming discrimination as a function of change in range rate

BASIC ASSUMPTIONS

The first consideration in range tracking through chaff dispensed by the target aircraft is in regard to the radar receiver AGC performance, since the interfering signal may well be ten times the amplitude of the signal being tracked. Taking the AN/APQ-50 airborne fire control radar as an example, for a step function input to the receiver AGC, the output has risen to approximately 10% of the final value in 5 prf periods. With the prf of 1200 pulses per second, this is a time of approximately 4 milliseconds. In estimating the significance of approximations used (Fig. 2), make a very conservative estimate of 0.1 second for total response time. Compare this with the range tracking bandwidth of approximately 1 radian/sec (corresponding to a response time of about 1 second). On the basis of at least a ten-to-one faster response time for the AGC loop (required to adequately control amplitude fluctuation for angle tracking) as compared with the range tracking loop response time, and not using results until approximately one second has elapsed after a transient, the assumption (conservative for the purposes of this analysis) may be made that the AGC is instantaneous in action against chaff return and that the conditions of Fig. 2 form a fair basis for analysis.

RANGE UNIT TRANSFER FUNCTION

The range unit transfer function shown on p. 41 of "Mechanization of the AN/APQ-50 Serial 15" (Confidential) by Westinghouse Corporation, Air Arm Division (23 December 1954), is closely related to the spectral energy distribution in the range tracking signal for the signal-to-noise ratio presented to the range unit at close range. The corresponding open-loop asymptotic plot is shown in Fig. 3.

The present study uses the transfer function referred to above as a design premise. The basic open-loop (OL) transfer function to be employed is given, using the notation of Fig. 3, by

$$\left.\frac{R_o}{R_i}\right|_{OL} = \frac{\omega_3\omega_8}{\omega_4} \frac{\omega_4 + s}{(\omega_1 + s)(\omega_3 + s)} = \mu \qquad (1)$$

[redacted]

UNCLASSIFIED

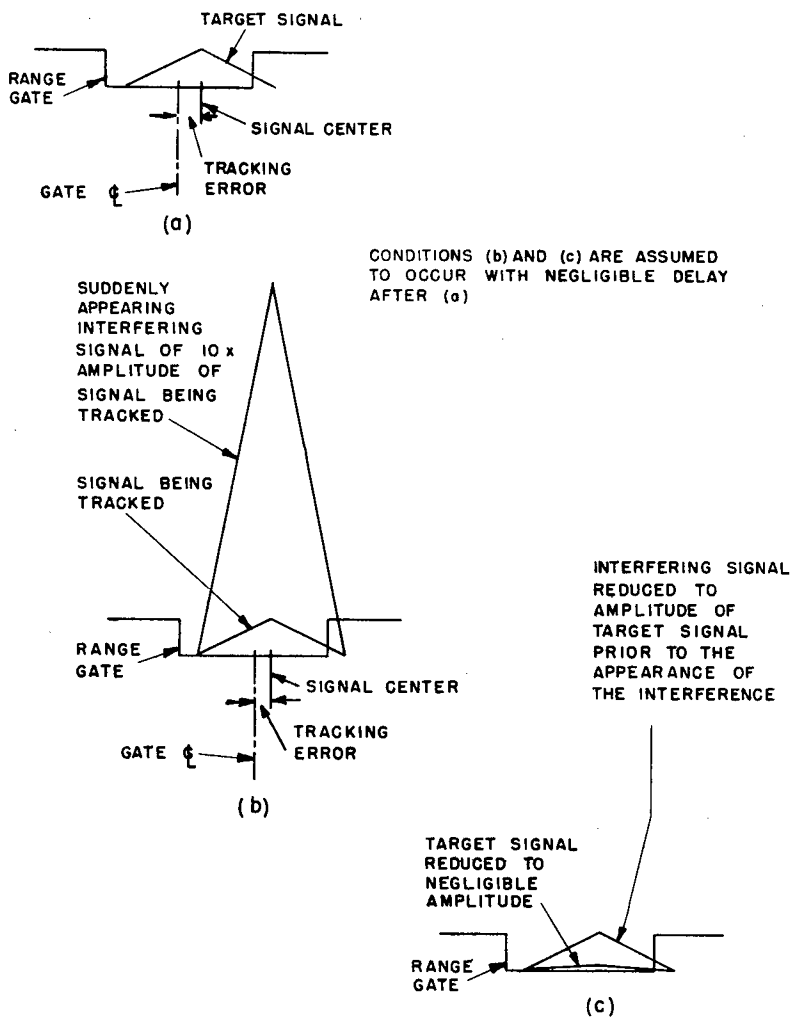

Fig. 2 - Assumptions for analysis of range tracking performance in the presence of chaff dispensed by the target

where

ω is the angular frequency in radians per second

s is the Laplace transform variable ($s = \sigma + j\omega$, $\sigma = 0$ for steady state).

The closed loop (CL) transfer function for $\beta = -1$ is

$$\left.\frac{R_o}{R_i}\right|_{CL} = \frac{\mu}{1+\mu} = \frac{\omega_3\omega_8(\omega_4 + s)}{\omega_4(\omega_1 + s)(\omega_3 + s) + \omega_3\omega_8(\omega_4 + s)}$$

$$= \frac{s\,\omega_3\omega_8 + \omega_3\omega_4\omega_8}{s^2\,\omega_4 + s(\omega_1\omega_4 + \omega_3\omega_4 + \omega_3\omega_8) + \omega_1\omega_3\omega_4 + \omega_3\omega_4\omega_8} \tag{2}$$

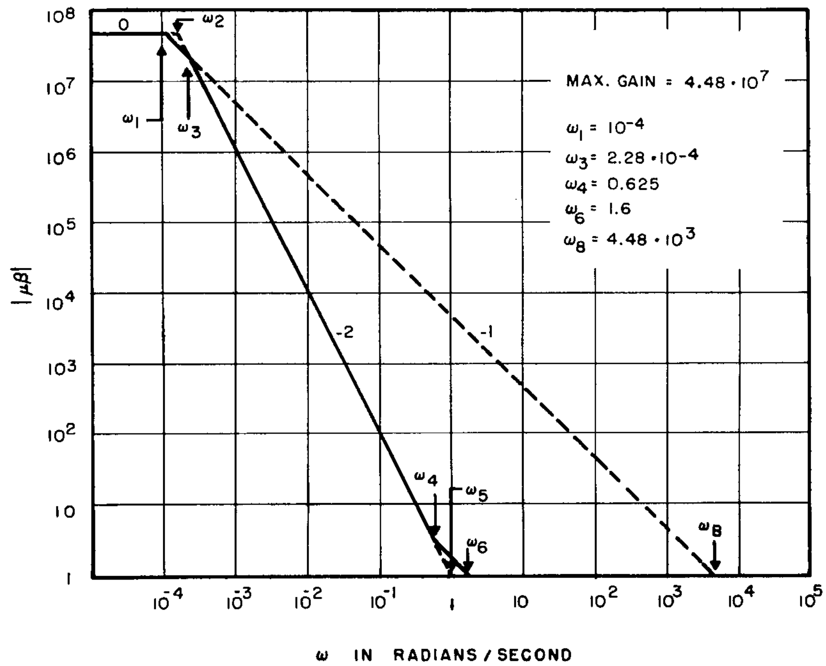

Fig. 3 - Range unit transfer function for S/N = +30 db

To reconstruct the closed-loop system function from the closed-loop transfer function, we rearrange Eq. (2) and take the inverse Laplace transform with the result

$$\begin{aligned} &\omega_4 \ddot{R}_o(t) + \left[\omega_1\omega_4+\omega_3\omega_4+\omega_3\omega_8\right] \dot{R}_o(t) + \left[\omega_1\omega_3\omega_4+\omega_3\omega_4\omega_8\right] R_o(t) \\ &\quad = \omega_3\omega_8 \dot{R}_i(t) + \omega_3\omega_4\omega_8 R_i(t). \end{aligned} \tag{3}$$

By taking the direct Laplace transform of Eq. (3), we obtain

$$\begin{aligned} &\omega_4\left[s^2R_o(s)-sR_o\big|_{o+}-\dot{R}_o\big|_{o+}\right] + \left[\omega_1\omega_4+\omega_3\omega_4+\omega_3\omega_8\right] \\ &\left[sR_o(s)-R_o\big|_{o+}\right] + \left[\omega_1\omega_3\omega_4+\omega_3\omega_4\omega_8\right] R_o(s) \\ &= \omega_3\omega_8\left[sR_i(s)-R_i\big|_{o+}\right] + \omega_3\omega_4\omega_8 R_i(s) \end{aligned} \tag{4}$$

and then by solving for $R_o(s)$, we obtain

$$R_o(s) = \frac{\left\{\begin{array}{l} s\left[\omega_4R_o\big|_{o+}+\omega_3\omega_8R_i(s)\right] + \left[\omega_4\dot{R}_o\big|_{o+}+(\omega_1\omega_4+\omega_3\omega_4+\omega_3\omega_8)R_o\big|_{o+} \right. \\ \left. -\omega_3\omega_8R_i\big|_{o+}+\omega_3\omega_4\omega_8R_i(s)\right] \end{array}\right\}}{s^2\omega_4 + s\left[\omega_1\omega_4+\omega_3\omega_4+\omega_3\omega_8\right] + \left[\omega_1\omega_3\omega_4+\omega_3\omega_4\omega_8\right]}. \tag{5}$$

[redacted]

UNCLASSIFIED

Examination of Eq. (5) shows that substitutions from the tactical problems must be made for $R_i|_{o+}$, $R_i(s)$, $R_o|_{o+}$, and $\dot{R}_o|_{o+}$ before further derivation.

Any particular tactical problem may be analyzed to find range as a function of time, indicated mathematically by

$$R_i(t) = f(t). \tag{6}$$

The function may be found unmanageable later in the Laplace transformation. In such an event, it may be expanded by use of Taylor's series

$$f(t) = a_o + a_1(t-t_o) + a_2(t-t_o)^2 + a_3(t-t_o)^3 + a_4(t-t_o)^4 + \ldots \tag{7}$$

where

$$a_o = f(t_o) \tag{8}$$

$$a_1 = f'(t_o) \tag{9}$$

$$a_2 = \frac{f''(t_o)}{2!} \tag{10}$$

$$a_3 = \frac{f'''(t_o)}{3!} \tag{11}$$

$$a_4 = \frac{f^{iv}(t_o)}{4!} \tag{12}$$

and where t_o is in the vicinity of the time of interest measured from the instant of chaff dispensing. Reserving a_1, a_2, etc., for the period prior to chaff dispensing $(t_o = 0)$, b_1, b_2, etc., for the period of chaff tracking (t_o is given a value estimated as the time at which $|\mathcal{E}_b| = 41$ yards), and c_1, c_2, etc., for subsequent target tracking, we expand $R_i(t)$ in a Taylor series in a manner similar to Eq. (7) and take the Laplace transform as follows:

$$R_i(t) = b_o + b_1(t-t_o) + b_2(t-t_o)^2 + b_3(t-t_o)^3$$
$$+ b_4(t-t_o)^4 + b_5(t-t_o)^5 + b_6(t-t_o)^6 + \cdots \tag{13}$$

$$= B_o + B_1 t + B_2 t^2 + B_3 t^3 + B_4 t^4 + B_5 t^5 + B_6 t^6 + \cdots \tag{14}$$

where

$$B_o = b_o - b_1 t_o + b_2 t_o^2 - b_3 t_o^3 + b_4 t_o^4 - b_5 t_o^5 + b_6 t_o^6 - \cdots \tag{15}$$

$$B_1 = b_1 - 2b_2 t_o + 3b_3 t_o^2 - 4b_4 t_o^3 + 5b_5 t_o^4 - 6b_6 t_o^5 + \cdots \tag{16}$$

[redacted]

$$B_2 = b_2 - 3b_3 t_o + 6b_4 t_o^2 - 10b_5 t_o^3 + 15b_6 t_o^4 - \dots \tag{17}$$

$$B_3 = b_3 - 4b_4 t_o + 10b_5 t_o^2 - 20b_6 t_o^3 + \dots \tag{18}$$

$$B_4 = b_4 - 5b_5 t_o + 15b_6 t_o^2 - \dots. \tag{19}$$

$$B_5 = b_5 - 6b_6 t_o + \dots \tag{20}$$

$$B_6 = b_6 - \dots \tag{21}$$

$$R_i(s) = \mathcal{L}\left[R_i(t)\right] \tag{22}$$

$$= \mathcal{L}\left[B_o + B_1 t + B_2 t^2 + B_3 t^3 + B_4 t^4 + B_5 t^5 + B_6 t^6 + \dots\right]$$

$$= \frac{B_o}{s} + \frac{B_1}{s^2} + \frac{2B_2}{s^3} + \frac{6B_3}{s^4} + \frac{24B_4}{s^5} + \frac{120B_5}{s^6} + \frac{720B_6}{s^7} + \dots \tag{23}$$

Returning to Eq. (5) and replacing $R_i(s)$ by the expression given in Eq. (23), we have the system output in s-domain as follows:

$$R_o(s) = \frac{\left\{\begin{aligned} & s\omega_4 R_o\big|_{o+} + \Big[\omega_3\omega_8 B_o + \omega_4 \dot{R}_o\big|_{o+} + (\omega_1\omega_4 + \omega_3\omega_4 + \omega_3\omega_8) R_o\big|_{o+} \\ & - \omega_3\omega_8 R_i\big|_{o+}\Big] + \frac{1}{s}\Big[\omega_3\omega_8 B_1 + \omega_3\omega_4\omega_8 B_o\Big] + \frac{1}{s^2}\Big[2\omega_3\omega_8 B_2 \\ & + \omega_3\omega_4\omega_8 B_1\Big] + \frac{1}{s^3}\Big[6\omega_3\omega_8 B_3 + 2\omega_3\omega_4\omega_8 B_2\Big] + \frac{1}{s^4}\Big[24\omega_3\omega_8 B_4 \\ & + 6\omega_3\omega_4\omega_8 B_3\Big] + \frac{1}{s^5}\Big[120\omega_3\omega_8 B_5 + 24\omega_3\omega_4\omega_8 B_4\Big] \\ & + \frac{1}{s^6}\Big[720\omega_3\omega_8 B_6 + 120\omega_3\omega_4\omega_8 B_5\Big] + \dots \end{aligned}\right\}}{s^2\omega_4 + s(\omega_1\omega_4 + \omega_3\omega_4 + \omega_3\omega_8) + (\omega_1\omega_3\omega_4 + \omega_3\omega_4\omega_8)}. \tag{24}$$

If it is assumed that sufficient terms have been indicated in the numerator of Eq. (24), we may write

$$R_o(s) = \frac{as^7 + bs^6 + cs^5 + ds^4 + es^3 + fs^2 + gs + h}{s^6\omega_4\left[s^2 - (s_1 + s_1^*)s + s_1 s_1^*\right]} \tag{25}$$

where

$$a = \omega_4 R_o\big|_{o+} \tag{26}$$

$$b = \omega_3\omega_8(B_o - R_i\big|_{o+}) + (\omega_1\omega_4 + \omega_3\omega_4 + \omega_3\omega_8) R_o\big|_{o+} + \omega_4 \dot{R}_o\big|_{o+} \tag{27}$$

[redacted]

UNCLASSIFIED

$$c = \omega_3\omega_8(B_1+\omega_4B_o) \tag{28}$$

$$d = \omega_3\omega_8(2B_2+\omega_4B_1) \tag{29}$$

$$e = 2\omega_3\omega_8(3B_3+\omega_4B_2) \tag{30}$$

$$f = \omega_3\omega_8(24B_4+6\omega_4B_3) \tag{31}$$

$$g = \omega_3\omega_8(120B_5+24\omega_4B_4) \tag{32}$$

$$h = \omega_3\omega_8(720B_6+120\omega_4B_5) \tag{33}$$

$$-(s_1+s_1^*) = \omega_1+\omega_3+\frac{\omega_3\omega_8}{\omega_4} \tag{34}$$

$$s_1s_1^* = \omega_3(\omega_1+\omega_8). \tag{35}$$

To facilitate the finding of the inverse Laplace transform of Eq. (25), we write the partial fraction expansion

$$R_o(s) = \frac{K_{11}}{s^6}+\frac{K_{12}}{s^5}+\frac{K_{13}}{s^4}+\frac{K_{14}}{s^3}+\frac{K_{15}}{s^2}+\frac{K_{16}}{s}+\frac{K_2}{s-s_1}+\frac{K_2^*}{s-s_1^*} \tag{36}$$

$$K_{11} = \left[\frac{as^7+bs^6+cs^5+ds^4+es^3+fs^2+gs+h}{\omega_4(s^2-\left[s_1+s_1^*\right]s+s_1s_1^*)}\right]_{s=0}$$

$$= \frac{h}{\omega_4s_1s_1^*} \tag{37}$$

$$K_{12} = \left[\frac{d}{ds}\;\frac{as^7+bs^6+cs^5+ds^4+es^3+fs^2+gs+h}{\omega_4(s^2-\left[s_1+s_1^*\right]s+s_1s_1^*)}\right]_{s=0}$$

$$= \frac{g}{\omega_4s_1s_1^*}+\frac{h(s_1+s_1^*)}{\omega_4(s_1s_1^*)^2} \tag{38}$$

$$K_{13} = \frac{1}{2}\left[\frac{d}{ds^2}\;\frac{as^7+bs^6+cs^5+ds^4+es^3+fs^2+gs+h}{\omega_4(s^2-\left[s_1+s_1^*\right]s+s_1s_1^*)}\right]_{s=0}$$

$$= \frac{f}{\omega_4s_1s_1^*}+\frac{g(s_1+s_1^*)-h}{\omega_4(s_1s_1^*)^2}+\frac{h(s_1+s_1^*)^2}{\omega_4(s_1s_1^*)^3} \tag{39}$$

[redacted]

$$K_{14} = \frac{1}{6}\left[\frac{d}{ds^3}\;\frac{as^7+bs^6+cs^5+ds^4+es^3+fs^2+gs+h}{\omega_4\left(s^2-\left[s_1+s_1^*\right]s+s_1s_1^*\right)}\right]_{s=0}$$

$$= \frac{e}{\omega_4 s_1 s_1^*} + \frac{f(s_1+s_1^*)-g}{\omega_4(s_1s_1^*)^2} + \frac{g(s_1+s_1^*)^2-2h(s_1+s_1^*)}{\omega_4(s_1s_1^*)^3} + \frac{h(s_1+s_1^*)^3}{\omega_4(s_1s_1^*)^4} \tag{40}$$

$$K_{15} = \frac{1}{24}\left[\frac{d}{ds^4}\;\frac{as^7+bs^6+cs^5+ds^4+es^3+fs^2+gs+h}{\omega_4\left(s^2-\left[s_1+s_1^*\right]s+s_1s_1^*\right)}\right]_{s=0}$$

$$= \frac{d}{\omega_4 s_1 s_1^*} + \frac{e(s_1+s_1^*)-f}{\omega_4(s_1s_1^*)^2} + \frac{f(s_1+s_1^*)^2-2g(s_1+s_1^*)+h}{\omega_4(s_1s_1^*)^3}$$

$$+ \frac{g(s_1+s_1^*)^3-3h(s_1+s_1^*)^2}{\omega_4(s_1s_1^*)^4} + \frac{h(s_1+s_1^*)^4}{\omega_4(s_1s_1^*)^5} \tag{41}$$

$$K_{16} = \frac{1}{120}\left[\frac{d}{ds^5}\;\frac{as^7+bs^6+cs^5+ds^4+es^3+fs^2+gs+h}{\omega_4\left(s^2-\left[s_1+s_1^*\right]s+s_1s_1^*\right)}\right]_{s=0}$$

$$= \frac{c}{\omega_4 s_1 s_1^*} + \frac{d(s_1+s_1^*)-e}{\omega_4(s_1s_1^*)^2} + \frac{e(s_1+s_1^*)^2-2f(s_1+s_1^*)+g}{\omega_4(s_1s_1^*)^3}$$

$$+ \frac{f(s_1+s_1^*)^3-3g(s_1+s_1^*)^2+3h(s_1+s_1^*)}{\omega_4(s_1s_1^*)^4}$$

$$+ \frac{g(s_1+s_1^*)^4-4h(s_1+s_1^*)^3}{\omega_4(s_1s_1^*)^5} + \frac{h(s_1+s_1^*)^5}{\omega_4(s_1s_1^*)^6} \tag{42}$$

$$K_2 = \left[\frac{as^7+bs^6+cs^5+ds^4+es^3+fs^2+gs+h}{\omega_4 s^6(s-s_1^*)}\right]_{s=s_1}$$

$$= \frac{as_1^7+bs_1^6+cs_1^5+ds_1^4+es_1^3+fs_1^2+gs_1+h}{\omega_4 s_1^6(s_1-s_1^*)} \tag{43}$$

$$K_2^* = \text{conjugate of } K_2. \tag{44}$$

In general we may set

$$K_2 = A_o + jD_o \tag{45}$$

$$K_2^* = A_o - jD_o \tag{46}$$

[redacted]

[redacted]

UNCLASSIFIED

$$s_1 = \sigma_o + j\omega_o \tag{47}$$

$$s_1^* = \sigma_o - j\omega_o . \tag{48}$$

The system output position as a function of time is

$$R_o(t) = \mathcal{L}^{-1}\left[R_o(s)\right]$$

$$= \mathcal{L}^{-1}\left[\frac{K_{11}}{s^6} + \frac{K_{12}}{s^5} + \frac{K_{13}}{s^4} + \frac{K_{14}}{s^3} + \frac{K_{15}}{s^2} + \frac{K_{16}}{s} + \frac{K_2}{s-s_1} + \frac{K_2^*}{s-s_1^*}\right] \tag{49}$$

$$= K_{16} + K_{15}t + \frac{K_{14}}{2}t^2 + \frac{K_{13}}{6}t^3 + \frac{K_{12}}{24}t^4 + \frac{K_{11}}{120}t^5 + K_2 e^{s_1 t} + K_2^* e^{s_1^* t} \tag{50}$$

$$= K_{16} + K_{15}t + \frac{K_{14}}{2}t^2 + \frac{K_{13}}{6}t^3 + \frac{K_{12}}{24}t^4 + \frac{K_{11}}{120}t^5 + 2\sqrt{K_2K_2^*}\, e^{\sigma_o t} \sin\left(\omega_o t + \tan^{-1}\frac{A_o}{-D_o}\right). \tag{51}$$

INTERFERING-SIGNAL TRACKING ERROR

The derivations have led to specification of the radar range unit output position, given by Eq. (51). The quantity of basic interest, however, is tracking error. This is given by

$$\epsilon_b(t) = R_i(t) - R_o(t). \tag{52}$$

Equation (13) is the expression for the input used in the process by which the output was found. The series expansion was used as an artifice facilitating the completion of the desired Laplace transformation. Here, however, the basic expression as derived from the flight path geometry of the tactical situation should be used to retain the greater available accuracy. Substitution of Eq. (51) into (52) yields

$$\epsilon_b(t) = R_i(t) - \left[K_{16} + K_{15}t + \frac{K_{14}}{2}t^2 + \frac{K_{13}}{6}t^3 + \frac{K_{12}}{24}t^4 + \frac{K_{11}}{120}t^5 + 2\sqrt{K_2K_2^*}\, e^{\sigma_o t} \sin\left(\omega_o t + \tan^{-1}\frac{A_o}{-D_o}\right)\right]. \tag{53}$$

In general, the maximum tracking error allowable, where the loss of target tracking is the criterion, is defined as one half the range gate width. For the AN/APQ-50 radar the gate width is 1/2 microsecond or 82 yards of range. Equation (53) is to be evaluated as a function of time. If a maximum error less than 41 yards is determined, the chaff has successfully caused the radar range unit to transfer from target tracking to chaff tracking.

[redacted]

If Eq. (53) shows tracking error continuing to increase without reaching a maximum by the time the magnitude of the error equals 41 yards, then the system has lost track on the interfering signal. The time of loss of track is $t = t_m$ where the following equality must be satisfied:

$$\Big[R_i(t)\Big]_{t_m} + 41 = K_{16} + K_{15}t + \frac{K_{14}}{2}t^2 + \frac{K_{13}}{6}t^3 + \frac{K_{12}}{24}t^4 + \frac{K_{11}}{120}t^5 + 2\sqrt{K_2K_2^*}\,e^{\sigma_o t}\sin\left(\omega_o t + \tan^{-1}\frac{A_o}{-D_o}\right). \tag{54}$$

If the system has lost track on the interfering signal, the question becomes one of determining whether the target is still within the gate. This is determined by evaluating

$$\mathcal{E}_{cT} = R_{iT}\Big|_{t_m} - \Bigg[K_{16} + K_{15}t_m + \frac{K_{14}}{2}t_m^2 + \frac{K_{13}}{6}t_m^3 + \frac{K_{12}}{24}t_m^4 + \frac{K_{11}}{120}t_m^5 + 2\sqrt{K_2K_2^*}\,e^{\sigma_o t_m}\sin\left(\omega_o t_m + \tan^{-1}\frac{A_o}{-D_o}\right)\Bigg] \tag{55}$$

where the subscript T in $\mathcal{E}_{cT}$ and R_{iT} refers to the target as distinguished from the chaff tracking where $\mathcal{E}_b$ and R_i have been used. The subscript c indicates that the c region as discussed immediately prior to Eq. (13) has been reached. Again, t_m corresponds to a 41-yard tracking error as computed from Eq. (53). If the error $\mathcal{E}_{cT}$ computed from Eq. (55) is less than 41 yards, the target is in the gate at the instant of loss of track of the chaff signal. The final question is whether, in continuing to track the target, the error will exceed 41 yards. If the maximum target track error exceeds 41 yards, the chaff was a successful countermeasure in that the radar range tracking is pulled off the target with the result that neither target nor interfering signal stay in the range gate. If the maximum target track error does not exceed 41 yards, the chaff has caused only a temporary disturbance to the range tracking in that target lock-on remains as the end result.

TARGET-TRACKING STEADY-STATE ERROR

The assumption is made that the error in tracking of the target prior to chaff dispensing may be accurately calculated using the steady state error series

$$\mathcal{E}_a = \frac{R_i}{K_p} + \frac{\dot{R}_i}{K_v} + \frac{\ddot{R}_i}{K_a} + \dots \tag{56}$$

$$\mathcal{E}_a\Big|_{o+} = \left[\frac{a_o}{K_p} + \frac{a_1}{K_v} + \frac{a_2}{K_a}\right]_{o+} \tag{57}$$

$$K_p = 1 + \frac{\omega_8}{\omega_1} \tag{58}$$

$$K_v = K_p\left(\frac{1 + \dfrac{\omega_1}{\omega_8}}{1 + \dfrac{\omega_1}{\omega_3} - \dfrac{\omega_1}{\omega_4}}\right)\omega_1 \tag{59}$$

[redacted]

UNCLASSIFIED

$$K_a = \frac{\omega_3^2\omega_4^2(\omega_1+\omega_8)^3}{\omega_8\begin{pmatrix}\omega_1\omega_3^2\omega_4+\omega_1\omega_3^2\omega_8+\omega_1^2\omega_3\omega_4+\omega_3\omega_4^2\omega_8\\ -\omega_1\omega_3\omega_4^2-\omega_1\omega_3\omega_4\omega_8-\omega_1^2\omega_4^2-\omega_3^2\omega_4^2-\omega_3^2\omega_4\omega_8\end{pmatrix}}. \qquad (60)$$

To determine the error in tracking the target after the chaff signal has left the gate, the same basic procedure previously developed must be used on essentially a new problem, since a sudden transient from the chaff input to target input occurs. The initial conditions for the new problem are derived from those obtaining at the instant the chaff tracking stops. To avoid confusion by further generalized derivations, a specific problem will now be considered.

COLLISION COURSE DYNAMICS

Figure 4 shows constant velocity target and interceptor courses with an angle α between the two headings. Chaff is dispensed at $t = 0$, which is t_c seconds before the projected collision of interceptor and target. The angle θ is the frequently required aspect angle of flight dynamics.

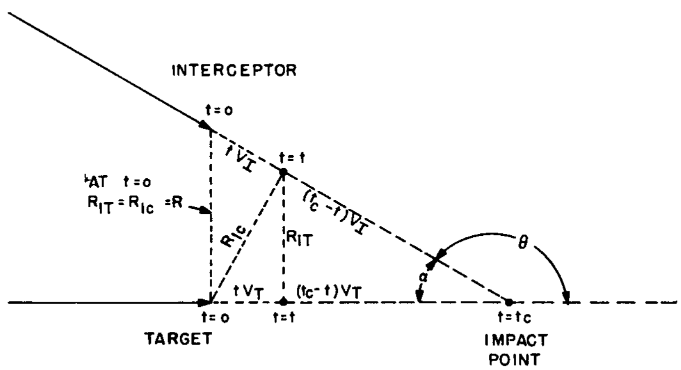

Fig. 4 - Collision course geometry

By consideration of the geometry of Fig. 4, the range from interceptor to target using the law of cosines is

$$R_{IT}^2 = (t_c-t)^2V_I^2 + (t_c-t)^2V_T^2 - 2(t_c-t)^2V_IV_T\cos\alpha \qquad (61)$$

$$= (V_I^2 - 2V_IV_T\cos\alpha + V_T^2)(t_c-t)^2. \qquad (62)$$

Introducing the ratio of interceptor to target speed as

$$R = \left|\frac{V_I}{V_T}\right| \qquad (63)$$

we have

$$R_{IT} = S_{IT}(t_c-t) \qquad (64)$$

[redacted]

where

$$S_{IT} = \left(V_I^2 - 2V_I V_T \cos\alpha + V_T^2\right)^{1/2} \tag{65}$$

$$= \left(R^2 - 2R \cos\alpha + 1\right)^{1/2} V_T. \tag{66}$$

Taking the derivative of Eq. (64), the range rate between interceptor and target is

$$\dot{R}_{IT} = -S_{IT}. \tag{67}$$

The range from interceptor to target may be expressed in the form indicated by Eq. (7) as follows:

$$R_{IT} = a_o + a_1 t \tag{68}$$

where

$$a_o = S_{IT} t_c \tag{69}$$

$$a_1 = -S_{IT}. \tag{70}$$

The time t_c is given by again using the law of cosines and Fig. 4. Thus,

$$R\Big|_{t=0}^2 = t_c^2 V_I^2 + t_c^2 V_T^2 - 2V_I V_T t_c^2 \cos\alpha \tag{71}$$

$$t_c = \frac{R\big|_{t=0}}{(V_I^2 - 2V_I V_T \cos\alpha + V_T^2)^{1/2}} \tag{72}$$

$$= \frac{R\big|_{t=0}}{\left|S_{IT}\right|}. \tag{73}$$

The range from interceptor to the chaff is given by

$$R_{Ic}^2 = (t_c - t)^2 V_I^2 + t_c^2 V_T^2 - 2t_c(t_c - t) V_I V_T \cos\alpha \tag{74}$$

$$= t^2 V_I^2 + t\left[2t_c V_I V_T \cos\alpha - 2t_c V_I^2\right] + \left[t_c^2 V_I^2 + t_c^2 V_T^2 - 2t_c^2 V_I V_T \cos\alpha\right] \tag{75}$$

$$R_{Ic} = \left[R^2 t^2 + 2R(\cos\alpha - R) t_c t + (R^2 - 2R\cos\alpha + 1) t_c^2\right]^{1/2} V_T \tag{76}$$

$$= \left[t^2 + \frac{2}{R}(\cos\alpha - R) t_c t + \left(1 - \frac{2}{R}\cos\alpha + \frac{1}{R^2}\right) t_c^2\right]^{1/2} V_I \tag{77}$$

$$= V_I\,(t^2 + Mt + N^2)^{1/2} \tag{78}$$

[redacted]

UNCLASSIFIED

where

$$M = \frac{2}{\mathcal{R}}(\cos\alpha - \mathcal{R})t_c \tag{79}$$

$$N^2 = \left(1 - \frac{2}{\mathcal{R}}\cos\alpha + \frac{1}{\mathcal{R}^2}\right)t_c^2 \tag{80}$$

$$= (\mathcal{R}^2 - 2\mathcal{R}\cos\alpha + 1)\frac{t_c^2}{\mathcal{R}^2} \tag{81}$$

$$= S_{IT}^2 \frac{t_c^2}{V_I^2} \tag{82}$$

$$N = S_{IT}\frac{t_c}{V_I}\,. \tag{83}$$

To express R_{Ic} in the series form of Eq. (13) we write

$$R_{Ic} = b_o + b_1(t-t_o) + b_2(t-t_o)^2 + b_3(t-t_o)^3 + b_4(t-t_o)^4 + b_5(t-t_o)^5 + b_6(t-t_o)^6 + \ldots \tag{84}$$

where, for

$$C = \left[t_o^2 + Mt_o + N^2\right]^{1/2} \tag{85}$$

and

$$G = 2t_o + M \tag{86}$$

the coefficients are defined as follows:

$$b_o = CV_I \tag{87}$$

$$b_1 = \frac{G}{2C}\,V_I \tag{88}$$

$$b_2 = \frac{4C^2-G^2}{8C^3}\,V_I \tag{89}$$

$$b_3 = \frac{G^3-4GC^2}{16C^5}\,V_I \tag{90}$$

$$b_4 = -\left(\frac{5G^4-24G^2C^2+16C^4}{128C^7}\right)V_I \tag{91}$$

$$b_5 = \left(\frac{7G^5-40G^3C^2+48GC^4}{256C^9}\right)V_I \tag{92}$$

[redacted]

$$b_6 = -\left(\frac{21G^6-140G^4C^2+240G^2C^4-64C^6}{1024C^{11}}\right)V_I. \tag{93}$$

NUMERICAL EXAMPLE

The AN/APQ-50 radar specifications call for tracking through interfering signals having 50 knots (or more) range rate differential with respect to the signal being tracked. If the collision course dynamics are used for an illustrative numerical example for an interceptor-target range of 3500 yards at the instant chaff is dispensed, and if the interceptor velocity is assumed to be 550 knots and the target velocity is taken as 500 knots, then a 50 knot or greater differential between interceptor-target range rate and interceptor-target dispensed chaff range rate occurs over a limited extent of values for α of Fig. 4. To derive the extent of the region of α, the absolute magnitude of the difference between $\dot{R}_{IT}$ (Eq. 67) and $\dot{R}_{Ic}$ (Eq. 78) gives

$$\left[\frac{\dot{R}_{IT}-\dot{R}_{IC}}{V_T}\right]_{t=0} = \frac{1-\mathfrak{R}\cos\alpha}{\sqrt{1-2\mathfrak{R}\cos\alpha+\mathfrak{R}^2}} \tag{94}$$

$$0.1 = \frac{1-1.1\cos\alpha}{\sqrt{1-2.2\cos\alpha+1.21}} \tag{95}$$

$$\alpha = \pm 30°59' \text{ and } \pm 19°29'. \tag{96}$$

To determine whether the AN/APQ-50 radar meets the specification under the conditions indicated above, we may proceed through the analysis in the sequence detailed in Table 1. We may now write an equation for error:

$$\begin{aligned}\mathcal{E}_b(t) = {} & 309.64(t^2-9.640t+127.772)^{1/2} \\ & -\Big[3481.980-134.884t+11.063t^2+0.455t^3 \\ & -0.00142t^4-0.00171t^5+2\times 12.815e^{-0.8173t} \\ & \sin\left(34.062t+\left[\tan^{-1}\left(\frac{9.0883}{-9.0348}=-1.00592\right)=134.833\right]\right)^{\circ}\Big].\end{aligned} \tag{97}$$

[redacted]

[redacted]

UNCLASSIFIED

TABLE 1
Sequence of Calculations

Quantity	Calculation Method	Numerical Value or Specialized Formula
ω_1	Fig. 3	10^{-4}
ω_3	Fig. 3	2.28×10^{-4}
ω_4	Fig. 3	0.625
ω_8	Fig. 3	4.48×10^3
$R_i\|_{o+}$	Problem statement	3500
$\mathcal{E}_a\|_{o+}$	Eq. (57) limited to this case	$\dfrac{a_o}{K_p} + \dfrac{a_1}{K_v}$
a_o	Problem statement	3500
a_1	Eq. (70)	$-S_{IT}$
$-S_{IT}$	Eq. (66)	
$\mathcal{R}$	Eq. (63), problem statement	1.1
α	Eq. (96), one limit	$30°59'$
a_1	Eq. (70), Eq. (66)	-160.20
K_p	Eq. (58)	4.48×10^7
K_v	Eq. (59)	3114.5
$\mathcal{E}_a\|_{o+}$	See above	-0.05
$R_o\|_{o+}$	Eq. (52), adapted	$R_i\|_{o+} - \mathcal{E}_a\|_{o+}$
$R_o\|_{o+}$	See above	3500.05
$\dot{R}_o\|_{o+}$	$= \dot{R}_o\|_{o-} = \dot{R}_i\|_{o-} = a_1$	-160.20
t_c	Eq. (73)	21.848
t_o	First estimate	2
M	Eq. (79)	-9.640
N^2	Eq. (82)	127.772
C	Eq. (85)	10.6062
G	Eq. (86)	-5.640
b_o	Eq. (87)	3284.104
b_1	Eq. (88)	-82.328

Table continues

[redacted]

TABLE 1 (continued)

Quantity	Calculation Method	Numerical Value or Specialized Formula
b_2	Eq. (89)	13.565
b_3	Eq. (90)	0.340
b_4	Eq. (91)	-0.01949
b_5	Eq. (92)	-0.001893
b_6	Eq. (93)	$+15.44 \times 10^{-6}$
B_o	Eq. (15)	3500.05
B_1	Eq. (16)	-132.038
B_2	Eq. (17)	11.212
B_3	Eq. (18)	0.4178
B_4	Eq. (19)	0.000366
B_5	Eq. (20)	-0.002078
B_6	Eq. (21)	+0.000015
a	Eq. (26)	2187.53
b	Eq. (27)	3475.735
c	Eq. (28)	2099.563
d	Eq. (29)	-61.388
e	Eq. (30)	16.876
f	Eq. (31)	1.6093
g	Eq. (32)	-0.2491
h	Eq. (33)	-0.1478
Quadratic	In denominator Eq. (25)	$s^2 + 1.6346s + 1.02144$
Quadratic	In denominator Eq. (25)	$(s - s_1)(s - s_1^*)$
s_1	Solution of quadratic	$-0.81732 + j\,0.59450$
s_1	Eq. (47)	$\sigma_o + j\omega_o$
s_1^*	Eq. (48)	$\sigma_o - j\omega_o$
s_1^2	Multiplication	$0.31457 - j\,0.97180$
s_1^3	Multiplication	$0.32063 + j\,0.98128$
s_1^4	Multiplication	$-0.84543 - j\,0.61140$

Table continues

[redacted]

UNCLASSIFIED

TABLE 1 (continued)

Quantity	Calculation Method	Numerical Value or Specialized Formula
s_1^5	Multiplication	1.05446 - j 0.00291
s_1^6	Multiplication	-0.86010 + j 0.62926
s_1^7	Multiplication	0.32888 - j 1.02564
$s_1 - s_1^*$	Substraction	+ j 1.18901
$s_1 + s_1^*$	Addition	-1.63463
$s_1 s_1^*$	Multiplication, $= \sigma_o^2 + \omega_o^2$	1.02144
K_{11}	Eq. (37)	-0.2315
$\frac{K_{11}}{120}$	Division	-0.001929
K_{12}	Eq. (38)	-0.01969
$\frac{K_{12}}{24}$	Division	-0.0008204
K_{13}	Eq. (39)	2.7790
$\frac{K_{13}}{6}$	Division	0.4632
K_{14}	Eq. (40)	22.0066
$\frac{K_{14}}{2}$	Division	11.0033
K_{15}	Eq. (41)	-134.098
K_{16}	Eq. (42)	3481.844
K_2	Eq. (43)	9.10916 + j 9.37515
K_2^*	Conjugate of K_2	9.10916 - j 9.37515
A_o	Real part K_2	9.10916
D_o	Imaginary part K_2	9.37515
$K_2 K_2^*$	Multiplication	170.870
$\sqrt{K_2 K_2^*}$	Square root	13.0717
$\mathcal{E}_b(t)$	Eq. (53)	contains $R_i(t)$
$R_i(t)$	Eq. (78)	$309.64\left[t^2-9.640t+127.772\right]^{1/2}$

[redacted]

By use of Eq. (97), the results of Table 2 are obtained. Since the expansion was performed around a time $t = t_o$, the values calculated have greatest accuracy in the neighborhood of $t_o = 2$ seconds. Accordingly, $t_m = 9.62$ seconds. Proceeding,

$$\begin{aligned} \mathcal{E}_{cT} &= R_{iT}\big|_{tm} - R_o\big|_{tm}, \quad \text{from Eq. (55)} \\ &= S_{IT}(t_c - t_m) - R_o\big|_{tm}, \quad \text{using Eq. (64)} \\ &= -1497.6 \text{ yd.} \end{aligned} \tag{98}$$

DISCUSSION OF NUMERICAL EXAMPLE

Since the chaff tracking error did not reach a maximum inside the allowable 41 yards absolute value, a time t_m corresponding to the maximum allowable range tracking error was computed and found to occur at $t_m = 9.62$ seconds after chaff was dispensed. The error between target range and range unit output was then computed at $t = t_m$ and found greatly in excess of the allowable maximum.

Thus, for the particular numerical example of an interceptor with a 550-knot speed on a collision course with a 500-knot target at $30°59'$ off the tail of the target, chaff dispensed at a range of 3500 yards caused temporary tracking of the chaff and eventual loss of both chaff and target.

SECOND NUMERICAL EXAMPLE

As a second numerical example, the same problem as that previously considered will be investigated with a change in the one parameter of differential range rate from the previously considered value of 50 knots to the much larger value of 300 knots. The same procedure used in the first numerical example gives the result

$$\mathcal{E}_{cT} = -12.27 \text{ yd.} \tag{99}$$

The value -12.27 yards computed for $\mathcal{E}_{cT}$ indicates that the range gate is lagging by an amount considerably less than the 41-yard maximum associated with loss of tracking. The question to be answered is whether the system will develop a maximum tracking error less than 41 yards and thereby continue tracking of the target. Proceeding as before, the results shown in Table 3 are obtained.

TABLE 2
Interfering-Signal Tracking Error

t (sec)	$\mathcal{E}_b$
2.5	26.1
3	27.0
5	29.9
9	35.7
9.5	39.7
9.6	40.8
9.62	41.0
10	45.8

TABLE 3
Target-Tracking Error After Loss of Interfering Signal

t (sec)	$\mathcal{E}_c$
0.80	-39.976
0.90	-40.326
1	-40.187
1.1	-39.693

[redacted]

UNCLASSIFIED

This second numerical example proves to be very close to the limiting case defining the minimum differential range rate for which the system will successfully ignore target dispensed chaff under the conditions of

Target velocity = 500 knots

Interceptor velocity = 550 knots

Course - Collision

Relative headings - α = 80°13′

J/S Ratio - Large

Interceptor to target range at instant chaff is dispensed = 3500 yards

Differential Range Rate = 300 knots.

The system returned to target tracking at 0.311 seconds after chaff was dispensed and maximum target tracking error of 40.33 yards lagging occurred at 1.211 seconds after chaff was dispensed.

The foregoing displays a formal analytical method whereby one point on a curve of the type shown in Fig. 1 can be found. A much more satisfactory procedure is a direct appeal to analog techniques that have the advantage of permitting introduction of system nonlinearities as well as the speed with which a wide range of parameter values may be investigated. However, within the framework of the analysis shown, other interference problems may be studied on an exploratory basis.

* * *

[redacted]

PART II - REPEAT-BACK JAMMING

INTRODUCTION

Repeat-back jamming is an electronic radar countermeasure in which a so-called range-gate-capture transponder is used to force the radar off the target by returning pulses that will enter the radar control circuits and convey false position information. Ordinarily, one transponder pulse is returned for each radar pulse received with the timing of the transponder pulses suitably varied to displace the radar range gate from the true target return. Developments in the field of repeat-back jamming have progressed to the point that the minimum delay between the leading edge of the received radar pulse and the beginning of the transponder reply pulse is small enough for operation against currently used radar range gate widths.

The object of the second part of the present study is to determine the time required for range gate pull-off as a function of factors determined by the J/S ratio. The availability of information regarding the ultimate lower limit of time required to deceive a given radar should assist in a realistic evaluation of the threat represented at any particular time by equipment currently employed.

The relative time delay between the radar pulse and the transponder reply may not be changed more rapidly than the radar range gate servo system can follow, if the range gate capture is to be successful. The problem is to construct an analog of an optimum transponder delay controller to permit calculations of the theoretical minimum time for pull-off.

BASIC ASSUMPTIONS

The radar range gate servo system transfer characteristic of the AN/APQ-50, used in the chaff study of Part I, is taken as typical of current airborne radar weapons control equipment and is used as the basis for study of the repeat-back jamming countermeasures technique.

Static tests of the AN/APQ-50 time discriminator indicate an error characteristic nearly linear within the gate width with a return to zero as shown in Fig. 5, Curve a. With the error characteristic shown, the gate must be made to lag the target echo by approximately a gate width before the correcting error voltage has dropped to zero. In a more modern receiver design employing either video or i-f pre-gating (as in the AN/APQ-50 of the present date) an error characteristic approximating the shape shown in Fig. 5, Curve b, is obtained under dynamic operating conditions. For the purposes of the present analysis, the linear error characteristic of Fig. 5, Curve c, is assumed. With the characteristic of Fig. 5, Curve c, the gate must be made to lag only one half a gate width before the correcting error voltage has dropped to zero. In actual practice, something intermediate between one-half and one gate width lag is required for successful interruption of range tracking. By presenting the calculated results in a normalized manner, the user is free to choose any amount of lag as a criterion for successful range gate capture.

The same assumption of complete replacement of the target echo by the transponder pulse as shown in Fig. 2 is made here. Thus, for a given initial delay between target echo and transponder pulse, the assumption is made of adequate J/S ratio to place enough jamming energy within the gate to cause the range discriminator error voltage to be determined

UNCLASSIFIED

entirely by the transponder pulse (i.e., the relative time position of the range gate and the transponder pulse). The magnitude of the usable initial transponder pulse delay is a function of the realizable J/S ratio. For large J/S ratio, large initial delays may be employed. By normalizing the initial delay with respect to the delay required to effect range gate capture, all J/S ratios are encompassed.

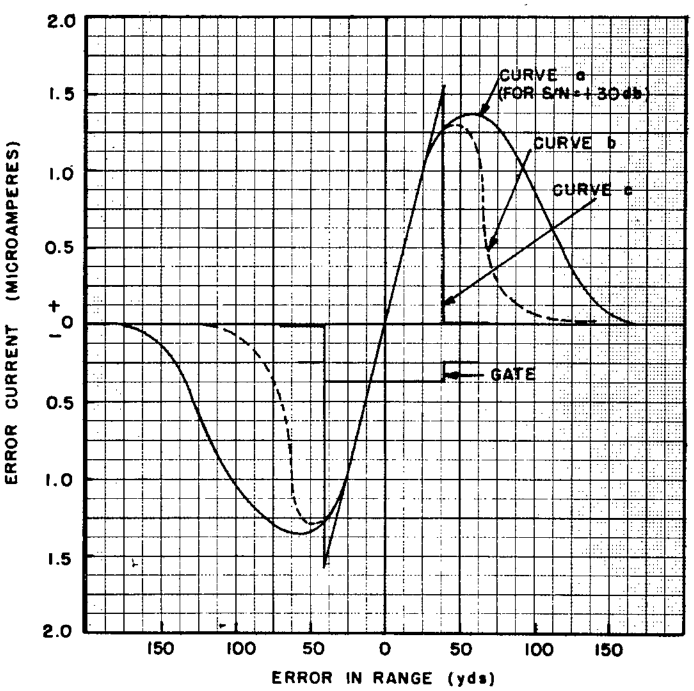

Fig. 5 - Time discriminator characteristics

OPTIMUM TRANSPONDER DELAY CONTROLLER

For a given J/S ratio, if the maximum permissible delay is used, an error voltage is obtained that drives the range gate toward the transponder pulse at a maximum rate. The response of the range servo system acts to reduce this error voltage. If the transponder pulse delay is increased at the same time, the range servo cannot reduce its error signal to zero. An optimum transponder delay controller is one that maintains the initial delay continuously as the range servo responds. Under these conditions, the range servo error signal remains unchanged as though its feedback loop were open. That is, the range servo input signal is not corrected by comparison with its output. With this concept of an optimum controller design, an analog can be formed as shown in Fig. 6. Added to the initial time delay between the target echo and the transponder pulse, shown as a step function of amplitude δ_I, is an increasing delay derived from application of the same step function to a filter having a transfer function matching the open-loop range servo transfer function.

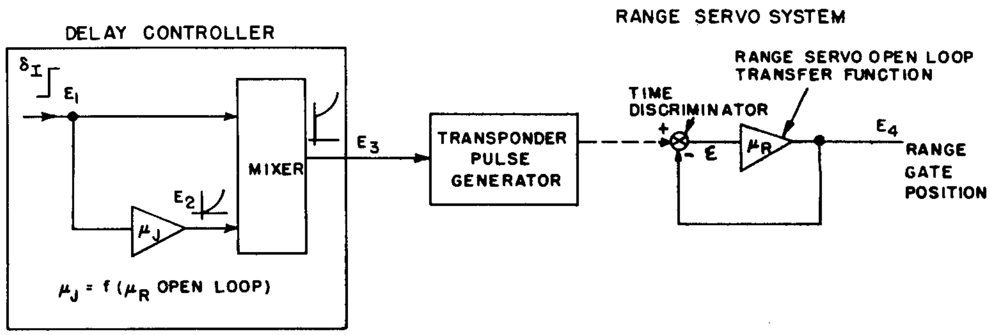

Fig. 6 - An optimum repeat-back jammer and a range servo system

CALCULATION OF RANGE-GATE-CAPTURE TIME

Referring to Fig. 6, the input E_1 represents the initial suddenly applied time delay which results in the sudden appearance of a range error ε. Using Laplace transform notation, we may write

$$E_1(t) = \delta_I, \quad t>o \tag{100}$$

$$E_2(t) = \mathcal{L}^{-1}\left[\frac{\delta_I}{s} \quad \mu_J\right] \tag{101}$$

$$E_3(t) = E_1 + E_2 = \delta_I \left[1+\mathcal{L}^{-1}\left(\frac{\mu_J}{s}\right)\right]. \tag{102}$$

The complex frequency domain equivalent of Eq. (102) becomes

$$E_3(s) = \mathcal{L}\left[\delta_I\left\{1+\mathcal{L}^{-1}\left(\frac{\mu_J}{s}\right)\right\}\right]. \tag{103}$$

The closed-loop response of the radar range servo system is given by

$$E_4 = \frac{\mu_R}{1 + \mu_R} E_3. \tag{104}$$

In general, the range servo error signal is

$$\varepsilon = \frac{1}{1 + \mu_R} E_3. \tag{105}$$

In the s-domain, using Eq. (103) to find E_3 and substituting in Eq. (105),

$$\varepsilon(s) = \frac{1 + \mu_J}{1 + \mu_R} \frac{\delta_I}{s}. \tag{106}$$

[redacted]

[redacted]

UNCLASSIFIED

Transforming to the time domain,

$$\mathcal{E}(t) = \mathcal{L}^{-1}\left[\frac{1+\mu_J}{1+\mu_R}\,\frac{\delta_I}{s}\right]. \tag{107}$$

The range servo output becomes equal to a general value δ_R at a time found from the general expression

$$E_4(t) = \mathcal{L}^{-1}\left[\frac{\mu_R}{1+\mu_R}\,(1+\mu_J)\,\frac{\delta_I}{s}\right] = \delta_R. \tag{108}$$

Let bandwidths be matched by setting $\mu_J = \mu_R$. Then

$$\mathcal{E}(t) = \delta_I \tag{109}$$

$$E_4(t) = \mathcal{L}^{-1}\left[\frac{\mu_R}{1+\mu_R}\,(1+\mu_R)\,\frac{\delta_I}{s}\right] = \delta_R. \tag{110}$$

$$\frac{\delta_R}{\delta_I} = \mathcal{L}^{-1}\left[\frac{\mu_R}{s}\right]. \tag{111}$$

Particularizing for the AN/APQ-50 radar,

$$\mu_R = \frac{\omega_3\omega_8}{\omega_4}\,\frac{\omega_4 + s}{(\omega_1 + s)(\omega_3 + s)} \tag{112}$$

so that Eq. (111) becomes

$$\frac{\delta_R}{\delta_I} = \mathcal{L}^{-1}\left[\frac{\omega_3\omega_8}{\omega_4}\,\frac{\omega_4+s}{s(\omega_1+s)(\omega_3+s)}\right] \tag{113}$$

$$= \frac{K_1}{s} + \frac{K_2}{s+\omega_1} + \frac{K_3}{s+\omega_3} \tag{114}$$

where

$$K_1 = \frac{\omega_8}{\omega_1} \tag{115}$$

$$K_2 = -\frac{\omega_3\omega_8}{\omega_4}\,\frac{\omega_4 - \omega_1}{\omega_1(\omega_3 - \omega_1)} \tag{116}$$

$$K_3 = \frac{\omega_8}{\omega_4}\,\frac{\omega_4 - \omega_3}{\omega_3 - \omega_1}. \tag{117}$$

[redacted]

Thus, Eq. (114) becomes

$$\frac{\delta_R}{\delta_I} = \frac{\omega_8}{\omega_1} - \frac{\omega_3\omega_8(\omega_4-\omega_1)}{\omega_1\omega_4(\omega_3-\omega_1)} e^{-\omega_1 t} + \frac{\omega_8(\omega_4-\omega_3)}{\omega_4(\omega_3-\omega_1)} e^{-\omega_3 t} . \tag{118}$$

Substituting numerical values for the parameters as given in Table 1,

$$\frac{\delta_R}{\delta_I} = 4.48\times10^7 - 7.9787232\times10^7 e^{-10^{-4} t} + 3.4987232\times10^7 e^{-2.28\times10^{-4} t} . \tag{119}$$

For an initial delay between target echo and transponder pulse of one-half gate width and the required range gate pull-off equal to one-half gate width, the ratio

$$\frac{\delta_R}{\delta_I} = 1 . \tag{120}$$

The time corresponding to $\delta_R/\delta_I = 1$ may be found indirectly by letting the time variable t in Eq. (119) have a range of values. Such calculations lead to the results plotted in Fig. 7 as the curve labeled $\omega_J = \omega_R$. Note that the inverse ratio δ_I/δ_R has been plotted to assist in a mental correlation with the J/S ratio. From the indicated curve,

$$\frac{\delta_I}{\delta_R} = 1 \quad \text{at } t \cong 0.58 \text{ seconds.} \tag{121}$$

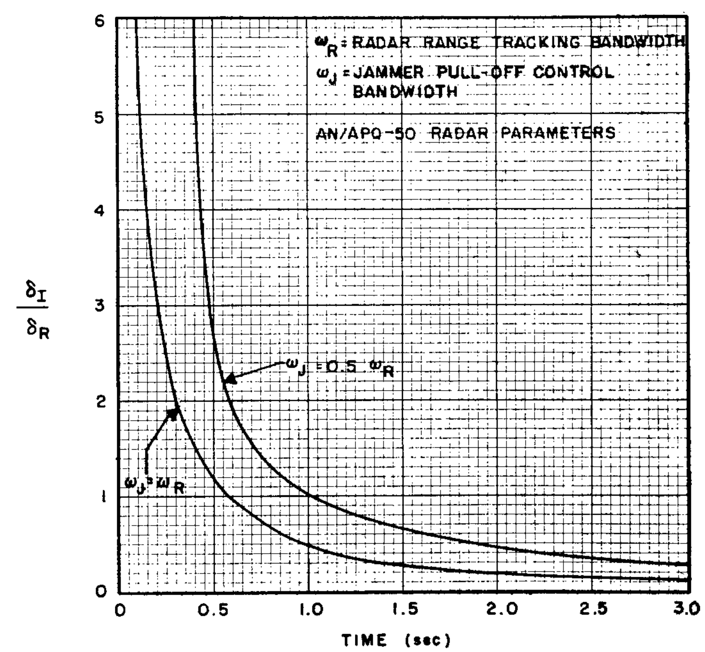

Fig. 7 - Repeat-back jamming range pull-off time for the AN/APQ-50 radar

[redacted]

[redacted]

UNCLASSIFIED

In a practical application of the concept developed here for the design of a transponder delay controller, the bandwidth of μ_J would be chosen somewhat lower than μ_R. To determine the increase over the theoretical minimum range gate pull-off times shown in the optimum design results on Fig. 7, curve $\omega_J = \omega_R$, another set of calculations was made letting the bandwidth of μ_J be half the bandwidth of μ_R, i.e., all values for ω_1, ω_3, ω_4, and ω_8 are to be made one octave lower. Then, using primes, the parameters have the values shown in Table 4. The results are shown on Fig. 7 by the curve labeled $\omega_J = 0.5\ \omega_R$.

TABLE 4
Jammer and Radar Parameters

μ_J		μ_R	
ω_1'	0.5×10^{-4}	ω_1	10^{-4}
ω_3'	1.14×10^{-4}	ω_3	2.28×10^{-4}
ω_4'	0.3125	ω_4	0.625
ω_8'	2.24×10^3	ω_8	4.48×10^3

GENERALIZED RANGE PULL-OFF RESULTS

Where the assumption can be made that a radar under study has the same range servo transfer function used in the AN/APQ-50 except for the actual numerical value of the bandwidth, a normalized replotting of Fig. 7 becomes useful. Thus, Fig. 8 becomes a valuable operational analysis tool in tactical studies. The bandwidth parameter ω_6 (in units of radians per second) can be given a value estimated for the radar under consideration to convert the dimensionless abscissa into units of seconds required for range gate capture.

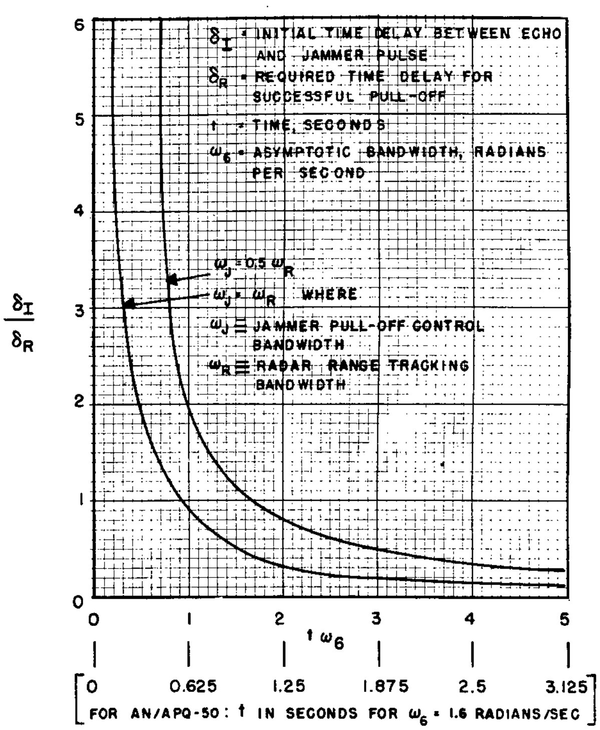

Fig. 8 - Generalized range pull-off time for repeat-back jamming

[redacted]

PULL-OFF VIA FALSE ANGLE INFORMATION

In addition to the previously discussed range gate pull-off, square-wave modulation can be superposed on the transponder pulse output to convey false angle information to the attacking radar. The envelope of the transponder pulses can be square-wave modulated at the lobing frequency of the radar antenna in such a phase as to cause the antenna to change direction and consequently lose the target. To accomplish angle deception, the output of the video detector in the jammer receiving equipment is amplified and the lobing modulation envelope is detected. A phase-shifter amplifier generates a square wave at the modulation frequency in which almost 180 degrees of control is available over the phase angle between the lobing modulation of the received signals and the square-wave output of the angle-deception circuits. Ordinarily, phase opposition to the modulation received is employed with an adjustable range available from -30 or -40 degrees to +140 or +130 degrees with respect to phase opposition.

CONCLUSIONS

Airborne radar vulnerability to the countermeasures of target-dispensed chaff and to repeat-back jamming may be determined using the standard analytical method of operational calculus and the radar range servo system transfer functions. The regions of vulnerability to target-dispensed chaff for a specific pure-collision tactical situation are established for the AN/APQ-50 airborne weapons-control radar.

The optimum design for a transponder delay controller is shown together with normalized curves of time to effect range-gate capture for various realizable jam-to-signal ratios. These results indicate the theoretical lower limit for pull-off time and the effect of less-than-optimum transponder delay controller design.

The relative significance of the extent of vulnerability as indicated in the present report can be established by comparison in an operations analysis with the tactical requirements for any projected employment of such weapons systems.

ACKNOWLEDGMENTS

Discussions with members of the Radar Division at the Naval Research Laboratory — especially those with Mr. Peter Waterman and members of the sections headed by Mr. L. F. Gilchrist, Mr. Howard Gordon, Jr., and Mr. S. F. George — materially aided the authors, particularly in the initial problem formulation. This work is a part of a more general study appearing as NRL Report 4949 ([redacted]), "Countermeasures and Antijam Considerations for Airborne Intercept Radars" ([redacted]) by L. F. Gilchrist, J. E. Abel, and J. C. Ryon.

* * *

[redacted]